

# Artificial Neural Network approach for assessment of residual compressive strength of geopolymer concrete exposed to elevated temperature

Sana D. Sayyad<sup>1</sup>, Hanmant S. Jadhav<sup>2</sup>

<sup>1</sup>Student M. Tech Structure, Rajarambapu Institute of Technology, Rajaramnagar

<sup>2</sup>Professor, Department of Civil Engineering, Rajarambapu Institute of Technology,  
Rajaramnagar

<sup>1</sup>sanasayyad0126@gmail.com

## Abstract

The population growth and industrial activities nowadays creates a considerable volume of rubbish, producing disposal challenges and major environmental hazards. The cement industry is a major generator of greenhouse gases like carbon dioxide. The use of waste resources, which avoids disposal worries while lowering greenhouse gases emissions into the atmosphere. This is a major reason for the advancement of cement-free Geopolymer Concrete. Fly ash (FA) and ground granulated blast furnace slag (GGBS) geopolymer concrete cubes were treated to various temperatures ranging from 27 °C to 800 °C in a 75:25 ratio. The mechanical properties were then evaluated. This study demonstrates the use of an Artificial Neural Network (ANN) approach to calculate the 28-day compressive strength of Geopolymer concrete (GPC) from input materials. 255 test examples from previously published studies were used for training, testing, and verifying the ANN model. Non-Destructive tests (NDT), Rebound Hammer (RH) and Ultrasonic pulse velocity (UPV) were done at the same curing age to confirm the compressive strength estimated by the Destructive test. A test project was also built to collect experimental data for testing the prediction capacity of the ANN model. According to the study's findings, the ANN model applying the "trainlm" learning strategy generated the highest predictive results. The unseen set of data had a prediction error of about 3.5MPa on average.

**Keywords:** compressive strength, elevated temperature, geopolymer concrete, artificial neural network

## 1. Introduction

The exponential expansion in population is increasing the demand for infrastructure. Because of its widespread usage adjacent to water, this need is negatively reflected in construction materials, notably Ordinary Portland Cement (OPC) (Sasi & Sumathy, 2021). The rise of urbanization and the global population increase have resulted in a 12% increase in global cement output in 2019, which is expected to quadruple by 2050. China dominates the worldwide cement industry, producing 2.4 billion tonnes in 2018, accounting for half of global cement consumption, followed by India, which produced 290 million tonnes. One tonne of cement may produce 0.6 to 1.0 tonne of CO<sub>2</sub> depending on the production process used, accounting for 59% of worldwide CO<sub>2</sub> emissions (Gunasekara, Atzarakis, Lokuge, Law, & Setunge, 2021). The environmental impact of cement on our ecosystem is quite severe, and it is hazardous to both human health and animals. It wastes natural resources and takes more energy to produce, in addition to emitting CO<sub>2</sub>. From an environmental standpoint, it has been determined that OPC utilization in the construction area has restrictions (T, Kannan, M, A, & R, 2021). As a result, finding a replacement binder from industrial by-products to complement OPC in concrete manufacture is crucial.

Several specialists have conducted extensive research on energy-efficient and ecofriendly construction materials during the last few decades. Geopolymers, as opposed to OPC, are produced utilizing aluminosilicate-rich natural materials and industrial wastes as the primary raw materials, instead of calcium carbonate calcination (CaCO<sub>3</sub>). CaCO<sub>3</sub> is the principal source of carbon dioxide emissions in the production of OPC. As a consequence, employing geopolymers can reduce greenhouse-gas emissions by 73% while also reducing energy use by 43%. It is possible to conclude that geopolymer binders will be a potentially feasible alternative to OPC for concrete manufacturing (Peng, et al., 2020).

Geopolymers are mostly made from geological materials with high strength and specialized characteristics. Geopolymer paste is an acceptable substitute for cement paste. Geopolymer binders work similarly to cement binders (bond strength, early high strength, thermal resistance, etc.) (Amin, Yara, Khaled, & Bassam, 2022). When compared to Portland cement (PC) binders, alkali-activated fly ash (AAF), also known as geopolymer, demonstrates substantial mechanical performance and structural stability under high temperature exposure. As a result, geopolymers have received the most attention in recent years in terms of fire resistance, enabling a wide range of uses such as fire-resistant material, heat insulators, and heat energy storage concretes. However, the energy-intensive elevated curing technique, as well as the inadequate initial strength, severely restrict the development of AAF's in-situ applications. To address these constraints, researchers are focusing on blended alkali-activated fly ash/GGBS binders (AAFS), which combine an aluminosilicate source (fly ash or metakaolin) with calcium additions. (Y, s, K, H, & Quigiang).

Davidovits coined the phrase "geopolymer concrete" (1978). For GC, many definitions have been offered. In 1978, Davidovits postulated that special binders may be incorporated by a polymeric reaction of geologically generated silicon and aluminum base material, which includes kaolin clay and alkaline liquids. Geopolymers are three-dimensional semi-

crystalline frameworks formed by mixing  $[\text{AlO}_4]^{-5}$  and  $[\text{SiO}_4]^{-4}$  tetrahedra. There are three types of calcium alkali-activated binders: lower content, higher content, and moderate content. Alkali activated binders are created by activating alkali materials based on aluminum silicates such as GGBFS, fly ash (FA), metakaolin (MK), and others (Kotha & A, 2020).

(Peng, et al., 2020) describes Geopolymer concrete (GPC) as a possible eco-friendly building material. Geopolymers are byproducts of polymerization processes that use aluminosilicate-rich materials and alkali activators. These raw materials include fly ash (FA), ground granulated blast-furnace slag (GGBFS), and metakaolin activators such sodium silicate ( $\text{Na}_2\text{SiO}_3$ , SS), and sodium hydroxide (NaOH, SH). GPC has the advantage of cement replacement (which is utilized in conventional concrete) with industrial waste. The GPC may utilize industrial byproducts as source materials, perhaps increasing sustainability dramatically. The geopolymer binder is an inorganic substance that is made by polymerizing aluminosilicate minerals with a strong alkaline solution. The polymerization process is divided into two parts. Stage I comprises the interaction of Al and Si atom from the raw material with hydroxide ions to produce geopolymer precursor ion (monomers). In Stage II, the precursors ion (monomers) polymerizes to form the three-dimensional geopolymer structure (Cao, Pilehvar, Juan, Thanh, & Carmona, 2018).

Buildings can sustain significant fire damage but protecting people and economic property is critical in all circumstances. There remains a chance of fire breaking out, despite technical breakthroughs and fire-control efforts. When subjected to high temperatures, ordinary concrete loses structural stability due to dehydration and the destruction of crystallized hydrates and C-S-H gel. Geopolymeric materials have an inherent fire resistance due to their inorganic framework; unlike organic polymers, they are very resistant to heat (Kotha & A, 2020).

In general, concrete has strong fire-resistant properties. However, because to dehydration and destruction of C-S-H and other crystalline hydrates, aggregate types, permeability, and other considerations, the strength properties of OPC concrete after a fire between 800 °C and 1000 °C is often less than 20%. Because fire produces a substantial difference in temperature, the hot layer of the body tends to split and spall out from cooler core layer. Geopolymers, on the other hand, have exceptional fire resistance at high temperatures due to the presence of extensively dispersed nano-pores in the ceramic-like microstructure, which allows physically and chemically linked water to travel and evaporate without destroying the aluminosilicate network (Singh, G, Gupta, & Bhattacharyya, 2015).

Because concrete structures are composite in nature, assessing the residual strength properties of concrete exposed to severe temperatures is a difficult task. Physical examination, in-situ laboratory testing, non-destructive, and partially destructive experimenting are all phases in assessing concrete after exposure to severe temperatures. There is no single assessment method that is superior to others. Multiple approaches may be necessary, and results must be carefully monitored at consistent residual strength levels. Traditional test methodologies used in normal conditions (e.g., destructive testing on core specimens) often do not account for the non-uniformity of concrete after a fire. NDT's key aims are to provide an immediate value of in-place strength of concrete to be used in structural capacity assessment or to detect internal faults in concrete members to help in

later adequacy evaluation. Ultrasonic pulse velocity (UPV) and rebound hammer testing are the most often used Non-Destructive Testing (NDT) methods for evaluating concrete properties (Schmidt Hammer). Interior cracks, voids, and other faults can also be identified using the ultrasonic pulse velocity method. The ultrasonic pulse velocity method was used to evaluate the structural integrity of high-temperature-heated concrete. The technique has advantages, such as a minimal effect on the building under consideration, a simple evaluation procedure, and the ability to analyze changes in the interior structure of concrete. Combining multiple NDT methodologies would result in a reasonable evaluation.

In this study, the compressive of Geopolymer concrete is evaluated using an approach of Artificial Neural Network (ANN). An artificial neural network is a sort of knowledge processing technology that is created by replicating the thinking and operating abilities of the human brain. A model of a real brain network is an artificial neural network. As a consequence, an artificial system that replicates the functioning of a biological neural systems will be built. The artificial neural network was made up of three parts: neurons, connection, and weights.

In this study, a supervised learning model is developed based on the ANN technique was developed to assess the compressive of GPC concrete at 28 days old. The structure of the ANN model was developed in MATLAB, with nine input parameters and one output. The ANN model was built in two stages utilizing different datasets. In the first stage, the ANN model was trained and validated using publicly available data from previous works. The second stage involved laboratory effort to gather experiment data for evaluating the prediction capability of the proposed ANN model. The suggested ANN model's non-destructive compressive strength test data were compared to the destructive testing of specimens' 28-day GPC compressive strength data.

## **2. Data Preparation**

### **2.1 Experimental data**

A total of fifteen GPC specimens were casted and tested in the lab at CSIR-CBRI, Roorkee, to establish the GPC 28-day compression strength. These specimens were ambient cured for 28 days prior to compression testing.

### **2.2 Materials**

**Fly-ash:** The starting material for this experiment was low-calcium (Class F) dry fly ash obtained from a nearby power plant. Burning bituminous or anthracite coals produces Class F fly ash. It contains less than 3% calcium (CaO) and more than 70% silica, alumina, and iron oxide.

**GGBS:** GGBS is a wasted product created by quenching molten iron from the furnace in steam or water, resulting in a granular and glassy substance that is dried and crushed into a fine powder. It contains calcium oxide, silica, alumina, and magnesia.

Fine aggregate: For fine aggregate, natural sand with a particle size of less than 4.75 mm was used.

Coarse aggregate: The coarse aggregate used are of 12.5mm and 20mm.

Alkaline solutions:

Sodium silicate: A local retailer will have silicate in solution form. The chemical compound sodium silicate is made up of sodium oxide, silica, and water. Sodium silicate is also known as water glass.

Sodium hydroxides: Sodium hydroxide, sometimes known as caustic soda and with the chemical formula NaOH, is a caustic metallic base that is available in pellets, flakes, granules, and a 50% saturated solution. To make the requisite concentration solution, sodium hydroxide pellets with a purity of 97-98% are acquired from a local store.

Chemical admixture: Sodium hydroxide, sometimes known as caustic soda, is a high range water reducing polycarboxylic ether-based new second generation superplasticizer concrete additive developed for concrete that demands high early and final strengths and durability.

### 2.3 Mix proportion

There is no standard mix design available for Geopolymer Concrete. There is relatively little research information available for a unique mix design strategy for FA-GGBS-based Geopolymer concrete. The rationale for this restricted study is because Geopolymer Concrete mix design is time-consuming and dependent on a variety of parameters. The mix design in this case was created by trial and error. Some of the components in the mix design were established as constants, while the others were adjusted per trial base. Table 1 illustrates the component mix proportions required.

**Table 1. Mix proportion of Geopolymer concrete**

Sr. No	FA (Kg/m <sup>3</sup> )	GGBS (Kg/m <sup>3</sup> )	NaOH (Kg/m <sup>3</sup> )	Na <sub>2</sub> SiO <sub>3</sub> (Kg/m <sup>3</sup> )	Fine aggregate (Kg/m <sup>3</sup> )	Coarse aggregate (Kg/m <sup>3</sup> )	
						20mm	12.5mm
1	310	102	55	135	750	570	570

### 2.4 Mixing

Initially, fine and coarse aggregates were generated for mixing under saturated dry surface conditions. The sodium hydroxide solution with the same molarity was kept ready for 24 hours prior to mixing to prepare the alkaline solution. This much time is necessary for the full breakdown of sodium hydroxide pellets in water as well as the liberation of heat from the created solution since the dissolving process is an exothermic reaction. Because the sodium silicate to sodium hydroxide solution ratio is 2.5, the produced NaOH solution was mixed with the sodium silicate solution. The mixing process was divided into two stages: dry mix and wet mix. The premixed FA

and GGBS were thoroughly mixed with fine and coarse aggregates in a saturated surface dry condition in the dry mix. The alkaline solution and superplasticizer were then gradually added to the dry mix, which was then wet mixed for approximately 4-5 minutes.

## **2.5 Casting and curing of geopolymer concrete**

Following the completion of the mixing, the required quantity of specimens for evaluating the various characteristics of Geopolymer Concrete were created in the corresponding moulds and vibrate for 1 minute on a vibrating table. The cast samples were destroyed after one day and left to cure at a temperature of  $27\pm 2^{\circ}\text{C}$ . 150mm cubes were evaluated for compressive strength after 28 days of curing, accordingly. For each test result, the overall strength is reported as the average of all three specimens.

## **2.6 Exposure specimens to high temperatures**

When the specimens attain the appropriate age, they are treated to temperatures of  $200^{\circ}\text{C}$ ,  $400^{\circ}\text{C}$ ,  $600^{\circ}\text{C}$ , and  $800^{\circ}\text{C}$ .

## **2.7 Non-destructive testing**

### **2.7.1 Ultrasonic pulse velocity test**

The Proceq Tico ultrasonic instrument is used to examine direct UPV data in concrete. This tester measures the propagation time of ultrasonic pulses in a sample with an accuracy of  $0.1\ \mu\text{s}$  and a range of  $0.1\text{-}9999.9\ \mu\text{s}$ . The transducers utilized had a diameter of 50mm and a maximum resonance frequency of 54kHz. Concrete cube specimens subjected to high temperatures with dimensions of  $150*150*150\ \text{mm}$  are measured. On 28 day-aged concrete blocks, ultrasonic pulse velocities were recorded using a pulse meter and an accompanying transducer pair in direct transmission mode. For appropriate acoustic connection, the concrete surface must be prepped, and grease applied ahead of time. Light pressure is required to ensure that the transducers make firm contact with the concrete surface. The pulse velocity of the Geopolymer Concrete samples was determined using IS 13311 (part 1:1992): 2004.

The ultrasonic pulse velocity measuring principle is to deliver a wave pulse into the concrete and time how long it takes for the pulse to travel through the concrete. The pulse is generated by a transmitter and detected by a receiver. For each concrete block, direct UPV measurements are collected at five separate sites, and the average results are derived. Knowing the route length, we can utilize the observed transit time( $t$ ) to determine the pulse velocity( $v$ ) as follows:

$$V=D/t$$

### 2.7.2 Rebound hammer test

The Rebound Hammer (RH) test (also known as the Schmidt hammer Test) is a non-destructive test invented by Ernst Schmidt, a Swiss Engineer, to determine the elastic characteristics or strength of concrete using the rebound principle. This equipment is used to assess direct UPV readings in concrete. The RH is largely a surface hardness tester, with little or no theoretical relationship between the rebound number (R) and concrete strength. Thus, empirical relationships between R and experimental concrete compressive strength (CS) are used to determine the CS of the tested concrete.

The Type N Schmidt test hammer complies with ASTM D5873 and has a simple menu-guided operation, electronic data processing, automatic correction for testing sites, and test data storage. The computerized processing of rebound and impact velocities enhances accuracy and repeatability. Battery life is anticipated to be 5000 hits or more between recharges. A Type N hammer has an impact energy of 2.207Nm. In this investigation, the Rebound Hammer test was done in line with IS13311 (part 2: 1992): 2004.

Before testing, the Schmidt hammer should be calibrated using the calibration chart that comes with it. During testing, the hammer measures the rebound of a spring-loaded mass (called R) as it strikes the surface of a testing sample. The energy released by the test hammer when it strikes the concrete surface is well defined. The rebound of the hammer is determined by the hardness of the material. RH measurements are made at six distinct points for each concrete cube, and the average values are determined. The conversion chart and the R are used to calculate the CS.

## 3. Artificial Neural Network Approach

In engineering, science, meteorology, economics, adaptive control, and robotics, the ANN is a common ML technique. Algorithms are traditionally built using fixed equation-based computations. As a result, when the quantity of input variables fluctuates often, they require a long time to calibrate. The equation's input and coefficient details must always be updated. To make things simpler, machine learning approaches were used. A supervised ML technique, such as ANN, does not have an exact equation, but it does necessitate a sufficient number of input and output variables. ANN can learn, recall, and generalize from the dependent and independent variables of a data set, and it can be re-trained with new data on a continuous basis.

Many studies have been completed using ANN to estimate the compression strength of concrete, and researchers are adopting this ML method to predict the desired outcome in other engineering fields. ANNs were developed to mimic the human brain. Because of its resemblance to the human brain, even the most basic and insignificant ANN possesses exceptional abilities in knowledge and information processing. As a result, an ANN might prove valuable in engineering applications.

Backward error propagation, sometimes known as backpropagation, is the most common training strategy for supervised ANN systems. This approach consists of two reversible phases, forward and backward. In the first stage, an arbitrary weight value is applied to

each connection in the whole network to establish the first link between input and output. During the second or backward phase, the difference (error) between the true and intended outputs is calculated and returned to the network. The connection weight is changed during these iterative methods to decrease input and output error. Despite the fact that it requires greater memory than other algorithms, Levenberg-Marquardt backpropagation is typically the fastest available backpropagation algorithm and is strongly recommended as a first-choice supervised approach.

### 3.1 Model Assessment

The performance of the ANN model was assessed using two criteria: coefficient of determination ( $R^2$ ) and Mean Squared Error (MSE).

### 3.2 Model Development

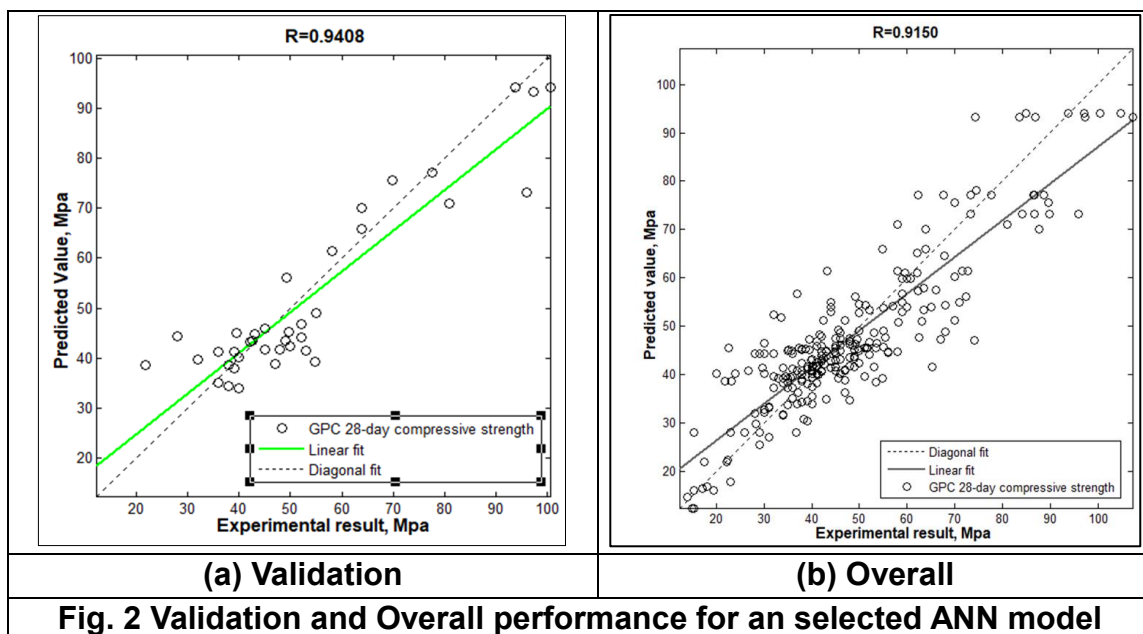
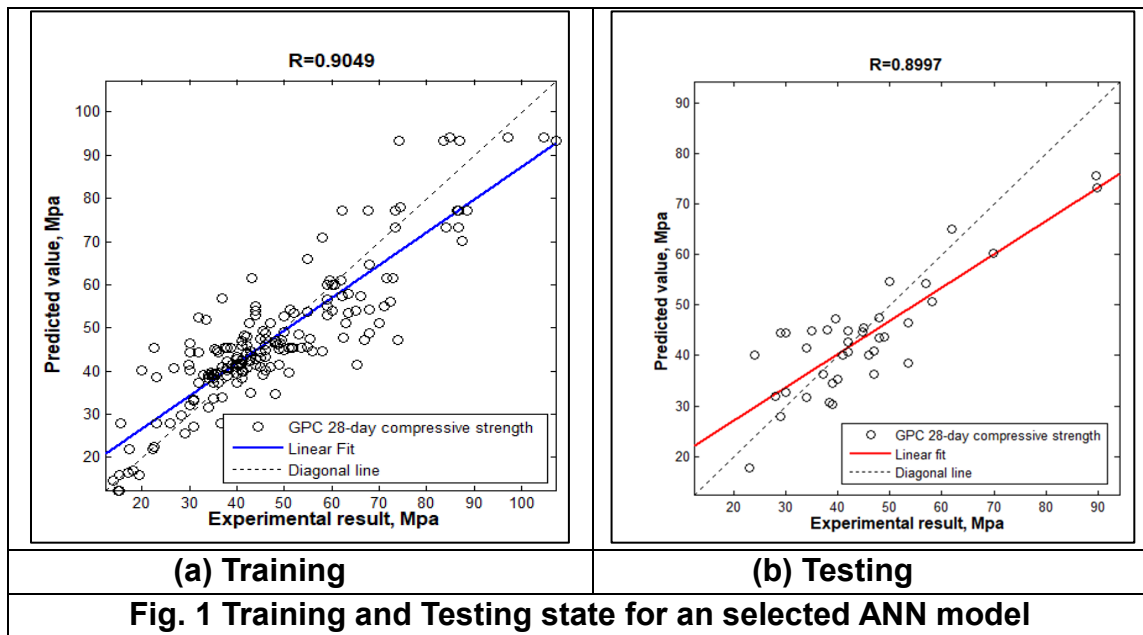
Temperature, fly ash, GGBS, fine aggregate, coarse aggregate, SH, SS, SH/SS ratio, and molarity data were all examined as input variables. For each of these input components, the 28-day compressive strength of concrete was obtained from existing literature. The number of input variables in the Artificial neural network model was chosen as nine, and the number of output variables was chosen as one, which means that 70%, or 179 specimens, were assigned to the training stage, 15%, or 38 specimens, were assigned to the validation (check) stage, and 15%, or 38 specimens, were assigned to the test stage out of the total selected number of 255 specimens.

Several training algorithms were evaluated, and the Levenberg Marquardt (LM) method was chosen as the best of the bunch. The prediction accuracy of the ANN model was evaluated using an experimental dataset of 15 data samples.

**Table 2. Details about the chosen ANN model**

Parameter	Information
# Neurons in the input layer	9
# Neurons in hidden layer	11
# Neurons in the output layer	1
Training method	backpropagation
Learning algorithm	trainlm
Activation function	sigmoid





## 4. Results and Discussion

### 4.1. Model Performance

The suggested ANN model, as previously indicated, was trained and validated using data from previously published research. Two indices were employed to assess the performance of the ANN model:  $R^2$  and MSE.

Regression charts are another technique to visualize the ANN model's performance outcomes. The suggested ANN model's performance results for datasets are presented in Figure. 1 and 2. In these graphs, the horizontal axis indicates the actual value, while the vertical axis displays the predicted values generated by the recommended ANN model.

The diagonal samples show the model's ideal forecast. Figure 1 depicts the relationship among experimental outcomes (target values) and anticipated values (output values) during the training and validation procedures.  $R^2$  is a statistical measure used to determine how near the data are to the fitted regression line. The model delivers good results in terms of R values in all figures.

### 4.2. Error Evaluation

Figure 3 depicts an error histogram of the proposed ANN model's performance errors divided into 20 bins (columns). The error was the difference between the ANN model's predicted and actual values. In this image, the vertical axis represents the number of samples from a dataset, while the horizontal axis represents the inaccuracy associated with the bins. The zero-line displays the zero inaccuracy of the horizontal axis. As can be seen, the majority of samples had errors ranging from -6.647 MPa to 10.76 MPa. The negative errors indicated that the anticipated value of the ANN model was smaller than the experimental value.

### 4.3. Application of Artificial Neural Network for Experimental Data

The compressive strength of the ANN model was then compared with the experimental compression strength obtained through destructive testing. The table displays the performance results of the model for the experimental data set. As demonstrated in Table 3, the ANN model performed admirably on the experimental dataset, with an average error of 3.5 MPa. It should be noted that the experiment dataset for the proposed ANN model was previously unknown. The ANN model could determine the compressive strength of GPC in a wide range from 22 MPa to 57 MPa with an estimated error of 20%. That is, the ANN model has the capability of generalizing the non - linear relationship between inputs and outputs.

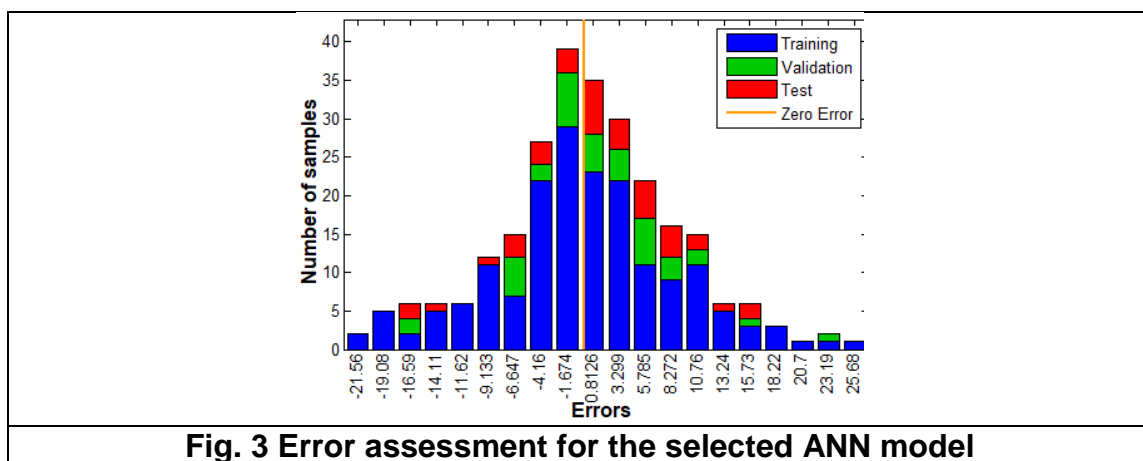


**Fig. 3 Error assessment for the selected ANN model**

**Table 3. Performance results for the proposed ANN model**

Experimental MPa	Predicted MPa	Error	Error%
56.040	59.559	3.519	6.280
50.400	41.192	9.208	18.270
53.330	43.730	9.600	18.001
60.490	63.371	2.881	4.763
79.020	76.258	2.762	3.496
53.470	55.848	2.378	4.447
49.330	48.706	0.624	1.265
52.760	52.326	0.434	0.823
47.330	47.358	0.028	0.059
35.690	32.449	3.241	9.082
31.260	31.168	0.092	0.294
30.440	30.529	0.089	0.294
25.420	19.613	5.807	22.844
20.180	20.165	0.015	0.072
22.710	22.700	0.010	0.042

## 5. Conclusions

The ANN technique was employed in this study to determine the compression strength of GPC at 28 days old. In the first stage, the ANN model was created using available data. In the second stage, the model's prediction capability was validated using experimental data. According to the results, the ANN model could predict a wide range of output for unknown experimental data with a 20% inaccuracy. Furthermore, the "trainlm" learning approach yielded the best results for the proposed ANN model. Finally, it was established that the ANN model might be used as an alternative method for reliably forecasting GPC compression strength.

Computational tests such as the mean squared error (MSE) and correlation coefficient (R) were used to establish the model's accuracy. In regression analysis, the linear equations were well matched to the experimental data obtained from preceding literatures and Non-Destructive test results. The coefficient (R<sup>2</sup>) value ranged from 0.89 to 0.99. For training, validation, and testing, the resulting R<sup>2</sup> value is near to one, indicating optimal fit.

According to the study's findings, geopolymers concrete manufacture should be encouraged in order to lessen the impact of global warming by successfully employing industrial byproducts and generating cement-free concrete.

The results of this work might help in the creation of a reliable soft computing tool for forecasting the compressive strength of concrete including blast-furnace slag and fly ash in a timely and precise way (supplementary materials). Once such a tool is carefully built, the prediction process can reduce the time and cost of experimental experiments.

## References

- [1] Ahmad, A., Ahmad, W., Chaiyasarn, K., Ostrowski, K. A., Aslam, F., Zajdel, P., & Joyklad, P. (2021), "Prediction of geopolymers concrete compressive strength using novel machine learning algorithms." *Polymers*, 13(19), 3389.
- [2] Annerel, E., & Taerwe, L. (2008), "Approaches for the assessment of the residual strength of concrete exposed to fire." *Concrete Repair, Rehabilitation and Retrofitting II*, 263-264.
- [3] Bilgehan, M. (2011), "A comparative study for the concrete compressive strength estimation using neural network and neuro-fuzzy modelling approaches." *Nondestructive Testing and Evaluation*, 26(01), 35-55.
- [4] Bui, D. K., Nguyen, T., Chou, J. S., Nguyen-Xuan, H., & Ngo, T. D. (2018), "A modified firefly algorithm-artificial neural network expert system for predicting compressive and tensile strength of high-performance concrete." *Construction and Building Materials*, 180, 320-333.
- [5] Chiang, C. H., & Chung-Chia, Y. (2005), "Artificial neural networks in prediction of concrete strength reduction due to high temperature." *ACI materials journal*, 102(2), 93.
- [6] Chopra, Palika, Rajendra Kumar Sharma, and Maneek Kumar (2016), "Prediction of compressive strength of concrete using artificial neural network and genetic programming." *Advances in Materials Science and Engineering*.
- [7] Dao, D. V., Ly, H. B., Trinh, S. H., Le, T. T., & Pham, B. T. (2019), "Artificial intelligence approaches for prediction of compressive strength of geopolymers concrete." *Materials*, 12(6), 983.
- [8] Hola, J., & Schabowicz, K. (2005), "Application of artificial neural networks to determine concrete compressive strength based on non-destructive tests." *Journal of Civil Engineering and Management*, 11(1), 23-32.
- [9] Huang, Q., Gardoni, P., & Hurlbaeus, S. (2011), "Predicting concrete compressive strength using ultrasonic pulse velocity and rebound number." *ACI Materials Journal*, 108(4), 403.
- [10] Ketabchi, H., Afshar, M. H., & Rasa, E. (2009), "Predicting Density and Compressive Strength of Concrete Cement Paste Containing Silica Fume Using Artificial Neural Networks." *Scientia Iranica*, 16(1).
- [11] Krishna, A. S., & Rao, V. R. (2019), "Strength prediction of geopolymers concrete using ANN." *International Journal of Recent Technology and Engineering*, 7, 661-667.
- [12] Karahan, O., Tanyildizi, H., & Atis, C. D. (2008), "An artificial neural network approach for prediction of long-term strength properties of steel fiber reinforced concrete containing fly ash." *Journal of Zhejiang University-SCIENCE A*, 9(11), 1514-1523.
- [13] Mai, H. V. T., Nguyen, T. A., Ly, H. B., & Tran, V. Q. (2021), "Investigation of ANN Model Containing One Hidden Layer for Predicting Compressive Strength of Concrete with Blast-Furnace Slag and Fly Ash." *Advances in Materials Science and Engineering*.
- [14] Nazari, A., & Torgal, F. P. (2013), "Predicting compressive strength of different geopolymers by artificial neural networks." *Ceramics International*, 39(3), 2247-2257.

- [15] *Suhaendi, S. L., & Horiguchi, T. (2006), "Effect of short fibers on residual permeability and mechanical properties of hybrid fiber reinforced high strength concrete after heat exposition." Cement and Concrete Research, 36(9), 1672-1678.*
- [16] *Toufigh, V., & Jafari, A. (2021), "Developing a comprehensive prediction model for compressive strength of fly ash-based geopolymer concrete (FAGC)." Construction and Building Materials, 277, 122241.*
- [17] *Julia Wróblewska, and Robert Kowalski (2020), "Assessing concrete strength in fire-damaged structures." Construction and Building Materials, 254, 119122.*
- [18] *Yang, H., Lin, Y., Hsiao, C., & Liu, J. Y. (2009), "Evaluating residual compressive strength of concrete at elevated temperatures using ultrasonic pulse velocity." Fire Safety Journal, 44(1), 121-130.s*
- [19] *Yang, D. S., Park, S. K., & Lee, J. H. (2003), "A prediction on mix proportion factor and strength of concrete using neural network." KSCE Journal of Civil Engineering, 7(5), 525-536.*